# Hybrid Convolution and Frequency State Space Network for Image Compression

Haodong Pan<sup>a</sup>, Hao Wei<sup>a</sup>, Yusong Wang<sup>a</sup>, Nanning Zheng<sup>a</sup>, Caigui Jiang<sup>a,\*</sup>

<sup>a</sup>State Key Laboratory of Human-Machine Hybrid Augmented Intelligence, National Engineering Research Center for Visual Information and Applications, and Institute of Artificial Intelligence and Robotics, Xi'an Jiaotong University, Xi'an, 710049, Shaanxi, China

#### Abstract

Learned image compression (LIC) has recently benefited from Transformerand state-space-model- (SSM-) based backbones. Convolutional neural networks (CNNs) excel at modeling local high-frequency details, whereas Transformer architectures capture long-range, low-frequency dependencies but suffer from quadratic complexity. State space models (SSMs) provide lineartime sequence modeling and are promising for capturing long-range visual dependencies; however, their direct application to images may cause structural information loss and ignores frequency characteristics that are crucial for compression. In this work, we propose a Hybrid Convolution and Frequency State Space Network (HCFSSNet) for LIC. HCFSSNet employs CNNs to extract local high-frequency structures and a Vision Frequency State Space (VFSS) block to model long-range low-frequency information. The VFSS block combines a Vision Omni-directional Neighborhood State Space (VONSS) module, which scans features along horizontal, vertical, and diagonal directions, with an Adaptive Frequency Modulation Module (AFMM) that leverages the discrete cosine transform to perform contentadaptive weighting of frequency components for more effective bit allocation. Furthermore, to reduce redundancy in the entropy model, we integrate AFMM with a Swin Transformer block to form a Frequency Swin Transformer Attention Module (FSTAM) for frequency-aware side-information mod eling. Experiments on the Kodak, Tecnick, and CLIC Professional Validation datasets show that HCFSSNet achieves competitive rate-distortion

<sup>\*</sup>Corresponding author. Email:cgjiang@xjtu.edu.cn

performance compared with recent learned image compression codecs, including SSM-based designs such as MambaIC, while using fewer parameters. In particular, HCFSSNet provides a compact and interpretable hybrid architecture that combines omni-directional visual state space modeling with fine-grained frequency-domain modulation, offering a favorable trade-off between compression efficiency, model complexity, and extensibility for future high-capacity designs. On Kodak, Tecnick, and CLIC, HCFSSNet reduces BD-rate over the VTM anchor by 18.06%, 24.56%, and 22.44%, respectively, while using 30-35% fewer parameters than recent SSM- and Transformer-based codecs such as MambaIC and MLIC++. The source code and models will be available at https://github.com/dongfengxijian/HCFSSNet.

## *Keywords:*

Learned image compression, Vision state space models, Frequency-domain analysis

#### 1. Introduction

Image compression is a critical problem in computer vision and multimedia applications, as it directly affects storage, transmission, and downstream visual analysis. Over the past few decades, traditional image compression techniques have undergone significant advances, resulting in widely adopted standards such as JPEG [1], JPEG2000 [2], WebP [3], BPG [4], and VVC [5]. However, these manually designed codecs often rely on hand-crafted transforms and heuristics, which makes it difficult to fully exploit complex statistical dependencies in natural images and often leads to suboptimal rate—distortion performance. With the rapid progress of deep learning in computer vision, learned image compression (LIC) algorithms have attracted increasing attention. Unlike traditional codecs, LIC methods [6, 7, 8] use end-to-end training to jointly optimize the analysis and synthesis transforms together with the entropy model, and have demonstrated superior rate—distortion performance compared with hand-designed standards, in line with classical rate—distortion theory [9].

Most LIC algorithms are built on an autoencoder framework [10], which typically comprises three key components: a nonlinear transform, quantization, and an entropy model. During encoding, the input image is mapped by a nonlinear analysis transform into a compact low-dimensional latent representation, which facilitates subsequent compression. The quantization opera-

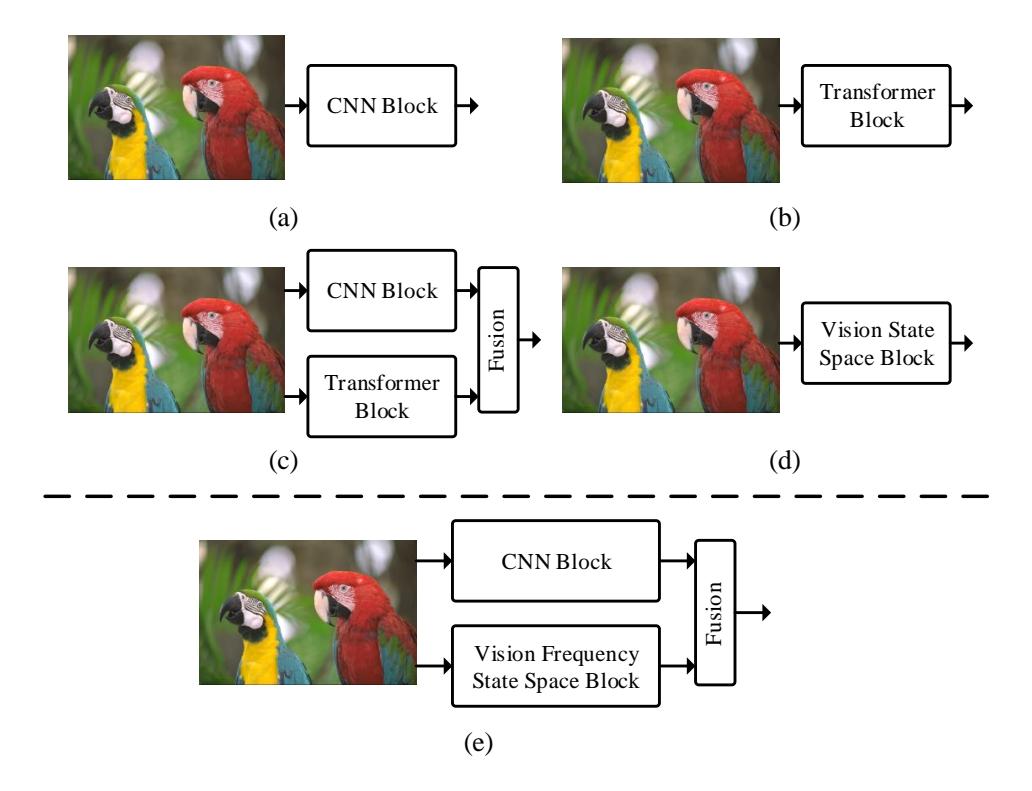


Figure 1: Representative nonlinear transforms used in learned image compression. (a) CNN-based methods (e.g., Chen et al. [13]); (b) Transformer-based methods (e.g., Zhu et al. [14]); (c) hybrid CNN-Transformer methods (e.g., Liu et al. [7]); (d) vision state space model (SSM)-based methods (e.g., Qin et al. [15]); and (e) the proposed HCFSSNet, which combines a CNN branch for local details with a Vision Frequency State Space (VFSS) branch for long-range dependencies.

tion discretizes this latent representation, while the entropy model estimates its probability distribution and compresses it into a bitstream via lossless entropy coding schemes, such as arithmetic coding [11] or range coding [12]). During decoding, the bitstream is entropy-decoded to recover the discrete latent representation, which is then mapped back to the reconstructed image by the synthesis transform.

Leveraging the feature-learning capacity of deep networks, recent LIC methods have mainly focused on the design of more powerful nonlinear transforms. As illustrated in Fig. 1, existing methods can be broadly categorized into four groups: (a) CNN-based methods, (b) Transformer-based methods

ods, (c) hybrid CNN-Transformer methods, and (d) vision state space model (SSM)-based methods.

(a) CNN-based methods: Chen et al. [13] introduced non-local attention modules to incorporate long-range dependencies into CNN-based compression networks. (b) Transformer-based methods: Zhu et al. [14] developed a Swin Transformer-based framework [16] for image and video compression, where window-based self-attention captures broader contextual information. (c) Hybrid CNN-Transformer methods: Liu et al. [7] proposed a parallel Transformer-CNN mixed block, in which CNNs capture fine-grained local details while Swin Transformers model long-range dependencies. (d) Vision SSM-based methods: Qin et al. [15] applied the recent Mamba architecture [17] to construct nonlinear transforms for image and video compression, demonstrating that SSMs provide strong long-range modeling capability with linear complexity.

Despite these advances, the aforementioned network designs still exhibit several limitations when applied to LIC. Transformer architectures, although effective at capturing non-local interactions, suffer from quadratic computational complexity with respect to the sequence length, which limits their scalability to high-resolution images. Mamba-style SSMs achieve linear-time long-range dependency modeling, but extending them from one-dimensional sequences to two-dimensional feature maps is non-trivial. Directly flattening feature maps into 1D sequences often disrupts the spatial neighborhood structure, and current vision SSM variants such as Vim [18], VMamba [19], and MambaIC [20] mainly rely on horizontal and vertical scan patterns. As a result, some important structural relationships—especially diagonal neighbors—may not be fully exploited, which is undesirable for compression-oriented representation learning.

In parallel with advances in network architecture design, another line of research has focused on improving entropy models for more accurate bitrate estimation. Hyperprior-based models [21, 22, 23, 8] employ 2D masked convolutions [24] or masked Transformers [25] to capture spatial dependencies in quantized latents, while 3D masked convolutions [26, 27] have been introduced to jointly explore spatial and cross-channel dependencies [28, 29, 30]. Furthermore, channel-wise autoregressive schemes [31] and spatial-channel context-adaptive models [32] have been proposed to reduce redundancy along both dimensions. Wang et al. [33] incorporated a hybrid attention mechanism into the channel entropy model to suppress low-frequency redundancy. However, most of these methods still operate primarily in the spatial and channel

domains. Simply decomposing latent features into low- and high-frequency components for separate processing may be overly coarse, and the side information in hyperprior-based models is seldom modeled in a frequency-aware manner. A more fine-grained analysis of different frequency components and content-adaptive bit allocation across them remains an important open problem.

In summary, existing CNN-, Transformer-, and SSM-based LIC frameworks, together with advanced spatial-channel entropy models, have significantly improved rate—distortion performance. Nevertheless, three key challenges remain: (1) current visual SSMs are not fully tailored to the structural characteristics of 2D images and may fail to capture important diagonal and omnidirectional neighborhood information; (2) most architectures do not explicitly decouple local high-frequency details from global low-frequency structures within a unified framework; and (3) entropy models rarely exploit frequency-domain representations of side information for fine-grained, content-adaptive bit allocation.

To address these challenges, we propose a novel learned image compression framework, the Hybrid Convolution and Frequency State Space Network (HCFSSNet). As shown in Fig. 1(e), HCFSSNet explicitly decouples local high-frequency and global low-frequency information in both the main transform and the entropy model. Along the main path, we design a Hybrid Convolution-Frequency State Space (HCFSS) block that splits feature channels into two branches: a CNN branch with small receptive fields to capture local details, and a Vision Frequency State Space (VFSS) branch that leverages state space models to handle long-range dependencies. To better adapt SSMs to two-dimensional images, the VFSS block incorporates a Vision Omni-directional Neighborhood State Space (VONSS) block, which scans features along horizontal, vertical, diagonal, and anti-diagonal directions to preserve complete local neighborhood structures. On top of this, an Adaptive Frequency Modulation Module (AFMM) operates in the discrete cosine transform (DCT) domain, enabling fine-grained, content-adaptive weighting of different frequency components and more efficient bit allocation. Furthermore, to reduce spatial redundancy in the side information of the entropy model, AFMM is integrated with a Swin Transformer block to form a Frequency Swin Transformer Attention Module (FSTAM), which performs frequency-aware modeling of the hyperprior features.

Very recently, learned image compression models such as MambaIC [20], DCAE [34], and LALIC [35] have further pushed the rate-distortion from-

tier by exploring state space and linear-attention architectures, dictionary-based cross-attention entropy models, and Bi-RWKV-based spatial—channel context modeling. Collectively, these methods represent the performance-oriented end of the design space: they achieve excellent BD-rate through complex sequence and context modules, with some of them incurring very large model sizes and computationally heavy entropy models.

The primary contributions of this work are summarized as follows:

- We propose a Hybrid Convolution and Frequency State Space Network (HCFSSNet) for learned image compression. HCFSSNet incorporates a Hybrid Convolution—Frequency State Space (HCFSS) block that explicitly splits features into a convolutional (CNN) branch for local high-frequency details and a Vision Frequency State Space (VFSS) branch that models global contextual information and long-range structures, which are typically dominated by low-frequency components.
- We develop a Vision Frequency State Space (VFSS) block that adapts state space models to two-dimensional feature maps via an omni-directional neighborhood scanning scheme (VONSS), preserving more complete structural information, including diagonal neighbors. VFSS further incorporates an Adaptive Frequency Modulation Module (AFMM) that operates in the DCT domain to perform fine-grained, content-adaptive weighting of different frequency components, leading to a more favorable rate-distortion trade-off.
- We design a Frequency Swin Transformer Attention Module (FSTAM) by integrating AFMM with a Swin Transformer block in the hyperprior path. FSTAM performs frequency-aware modeling of the hyperprior features, effectively reducing spatial redundancy in side information and improving the modeling capability of the channel-wise entropy model.
- We conduct comprehensive experiments and ablation studies on the Kodak, Tecnick, and CLIC Professional Validation datasets. The results show that HCFSSNet consistently improves BD-Rate over the conventional VTM anchor and achieves rate-distortion performance close to that of recent SSM-based codecs such as MambaIC [20], while using about 30–35% fewer parameters. At the same time, HCFSSNet consistently outperforms representative CNN- and Transformer-based LIC

baselines across all three benchmarks, and yields clear gains over the frequency-aware FTIC codec on high-resolution datasets.

#### 2. Related Work

## 2.1. Learned Image Compression

Learned image compression (LIC) has significantly outperformed traditional handcrafted codecs in terms of rate—distortion performance and has therefore attracted substantial attention in recent years. This success is primarily attributed to two key components: (i) powerful nonlinear transforms that learn compact representations and (ii) accurate entropy models for precise bitrate estimation. In this subsection, we briefly review related work on nonlinear transforms and entropy models.

# 2.1.1. Nonlinear Transform

Neural networks have demonstrated strong nonlinear modeling capabilities in visual tasks, thereby motivating many researchers to replace traditional hand-crafted modules in image codecs with learned transforms. Ballé et al. [36] introduced a convolutional autoencoder with generalized divisive normalization (GDN) layers as the nonlinear transform, marking one of the first end-to-end CNN-based image compression frameworks. Chen et al. [28] incorporated a non-local attention module to adaptively allocate bits to informative features, thereby improving the representation of important structures and enhancing the rate-distortion trade-off. Tang et al. [30] integrated graph attention mechanisms with asymmetric CNNs to jointly capture both short- and long-range dependencies. Zhang et al. [37] proposed a decoupled architecture that separates bitstream parsing from latent reconstruction, significantly reducing decoding time while maintaining competitive compression efficiency.

The Transformer [38] architecture has achieved remarkable success in computer vision, and several LIC methods have explored Transformer-based nonlinear transforms. Zhu et al. [14] designed a Swin Transformer-based framework for both image and video compression, where window-based self-attention effectively models long-range dependencies. Zou et al. [39] developed a simple yet effective local attention module to enhance CNN-based compression networks. Lu et al. [40] and Liu et al. [7] combined Swin Transformers with convolutions to jointly exploit long-range and local information. Wang et al. [41] proposed an adaptive scheme that decomposes features into

low- and high-frequency components, which are then processed by an invertible CNN block and a Swin Transformer—based hybrid attention block, respectively. Ge et al. [42] introduced contextual sequential quantization to progressively discretize latent features by leveraging contextual information and textural priors.

More recently, state space models (SSMs) have become a highly active research topic in computer vision. Motivated by the strong long-range modeling capability and linear-time complexity of Mamba [43], Qin et al. [15] proposed MambaVC, an image and video compression framework that replaces convolutional and attention blocks in a conventional LIC backbone with Mamba blocks. Zeng et al. [20] further developed an SSM-based LIC framework, MambaIC, which integrates visual state space blocks not only into the main analysis and synthesis transforms but also into the hyperprior and context modules, achieving a better trade-off between rate-distortion performance and latency, especially for high-resolution images. In parallel, vision SSM variants such as Vim [18] and VMamba [19] have been proposed to extend 1D SSMs to 2D feature maps, typically by scanning features along horizontal and vertical directions. Xiao and Xia [44] proposed a pixel adaptive deepunfolding network that combines CNNs with state space models for image deraining, demonstrating that SSMs can efficiently capture long-range dependencies with linear complexity while being fused with frequency-domain features via Fourier transforms.

Very recently, several high-performing LIC frameworks have been proposed, including MambaIC [20], DCAE [34], and LALIC [35]. MambaIC integrates visual state space blocks throughout both the main and hyperprior transforms, forming a deep SSM-driven architecture with excellent rate—distortion performance. DCAE introduces a dictionary-based cross-attention entropy model with multi-scale feature aggregation, which significantly strengthens probability estimation at the cost of a computationally heavy entropy module and a large overall model size (about 119M parameters). LALIC, in contrast, is a linear-attention-based codec built upon Bi-RWKV blocks with Spatial-Mix and Channel-Mix and an RWKV-based spatial—channel context model, leveraging efficient linear attention and Omni-Shift convolutions to achieve competitive BD-rate with a moderate parameter budget (around 63M parameters) and decoding latency.

Our HCFSSNet is complementary to these high-performing systems: rather than relying on increasingly heavy entropy models or sequence modules, it focuses on a unified hybrid convolution—frequency-SSM architecture that couples omni-directional visual state space modeling with frequency-domain modulation in both the main transform and the entropy model. This design keeps the model relatively compact while still delivering competitive rate—distortion performance and providing an interpretable building block for future large-capacity codecs.

These works demonstrate that CNNs, Transformers, and SSMs can all serve as effective nonlinear transforms for LIC. However, most existing SSM-based designs directly adopt 1D scan patterns, which can disrupt or only partially preserve the 2D neighborhood structure (e.g., diagonal neighbors). In addition, they seldom exploit fine-grained frequency characteristics that are crucial for compression-oriented representation learning.

## 2.1.2. Entropy Model

Another major line of research in LIC focuses on designing more effective entropy models to accurately estimate the prior distribution of quantized latent features. Eliminating spatial redundancy has been a primary approach to improving entropy coding efficiency. Ballé et al. [45] introduced a hyperprior model to capture spatial dependencies in latent representations, significantly enhancing rate—distortion performance. Minnen et al. [21] showed that autoregressive and hierarchical priors are complementary and demonstrated the benefits of combining them. To alleviate the sequential decoding bottleneck of autoregressive models, He et al. [46] proposed a checkerboard context model that enables parallel decoding over disjoint subsets of spatial positions. Recently, Wang et al. proposed S2LIC [47], which integrates SwinV2-based transforms with an adaptive channel-wise and global-inter attention context (ACGC) entropy model to further improve rate—distortion performance.

Reducing channel redundancy has also become an important research direction in LIC. Mentzer et al. [29] proposed a 3D CNN-based entropy model to more effectively capture cross-channel dependencies. Minnen et al. [31] introduced a channel-wise autoregressive entropy model that partitions latent features into channel slices and predicts each slice conditioned on previously decoded ones. Building on these efforts, several works have explored joint spatial—channel entropy modeling. He et al. [32] developed an unevenly grouped spatial—channel contextual adaptive entropy model that simultaneously leverages spatial and channel correlations. Li et al. [48] partitioned latent features into groups along both spatial and channel dimensions and then applied entropy coding to these groups using a grouped context model,

further reducing redundancy. Other methods have incorporated hybrid attention mechanisms or region-of-interest priors into the entropy model to better match the statistics of structured content such as edges or salient regions.

Overall, existing entropy models have significantly improved the accuracy of probability estimation by exploiting spatial, channel, and hyperprior information. However, most methods operate primarily in the spatial and channel domains, and the side information in hyperprior-based models is rarely modeled in a frequency-aware manner. Fine-grained, content-adaptive bit allocation across different frequency components of both the latents and the side information remains underexplored.

## 2.2. Frequency-aware Image Compression

Frequency-domain analysis has long been a cornerstone of traditional image compression. Classical codecs such as JPEG, JPEG2000, WebP, and BPG rely on transforms such as the discrete cosine transform (DCT) or the discrete wavelet transform (DWT) to convert images from the spatial domain to the frequency domain, where high- and low-frequency components can be processed separately. This separation facilitates the design of quantization strategies that exploit the varying perceptual importance of different frequency bands.

Recently, frequency-aware modeling has also been introduced into learned image compression and related visual tasks. Yao et al. [49] proposed Wavelet Vision Transformer (Wave-ViT), which uses the discrete wavelet transform (DWT) to downsample Keys and Values in Transformers, reducing computational complexity while preserving accuracy. Li et al. [8] introduced a frequency-decomposition window attention mechanism to capture anisotropic frequency components in images, together with a frequency-modulation feedforward network that adaptively integrates different frequency components. Wang et al. [33] employed a dynamic frequency filter to decompose features into low- and high-frequency components, which are processed separately by a hybrid attention block and an invertible neural network block, respectively, thereby reducing redundancy in low-frequency channels while preserving high-frequency details. Tang et al. [50] proposed a spatial—frequency hybrid restoration network that employs dual branches in the spatial and frequency domains to better handle JPEG-induced artifacts and blur, highlighting the benefit of explicitly modeling complementary spatial and frequency information.

Although these methods demonstrate the benefits of incorporating frequency-domain priors into learned image compression, most of them either perform a relatively coarse separation into low- and high-frequency components or treat frequency-domain operations as auxiliary modules decoupled from the main architecture. In addition, frequency-domain modeling of the hyperprior or side information in entropy models has received limited attention. In contrast, our work leverages DCT-based frequency modulation not only in the main transform, where it is tightly coupled with a Vision Frequency State Space branch, but also in the hyperprior path, where it guides frequency-aware side-information modeling. This design enables fine-grained, content-adaptive weighting of different frequency components and leads to more efficient rate-distortion trade-offs.

#### 3. Method

## 3.1. State Space Model Preliminaries

State space models (SSMs) are classically formulated as linear time-invariant (LTI) systems that map a one-dimensional input signal  $x(t) \in \mathbb{R}$  to a one-dimensional output signal  $y(t) \in \mathbb{R}$  via an n-dimensional hidden state  $h(t) \in \mathbb{R}^n$ . The continuous-time dynamics can be described by the following linear ordinary differential equation (ODE):

$$h'(t) = \mathbf{A}h(t) + \mathbf{B}x(t),$$
  

$$y(t) = \mathbf{C}h(t) + \mathbf{D}x(t),$$
(1)

where  $\mathbf{A} \in \mathbb{R}^{n \times n}$  is the state matrix,  $\mathbf{B} \in \mathbb{R}^{n \times 1}$  is the input (or control) matrix,  $\mathbf{C} \in \mathbb{R}^{1 \times n}$  is the output matrix, and  $\mathbf{D} \in \mathbb{R}$  is the feed-through term. All these parameters are learnable and can be optimized via gradient backpropagation.

To adapt Eq. 1 for practical deep learning applications, the zero-order hold (ZOH) rule is applied to discretize the continuous system. The matrices **A** and **B** are discretized as

$$\overline{\mathbf{A}} = \exp(\Delta \mathbf{A}),$$

$$\overline{\mathbf{B}} = (\Delta \mathbf{A})^{-1} (\exp(\Delta \mathbf{A}) - \mathbf{I}) \cdot \Delta \mathbf{B},$$
(2)

where  $\Delta$  denotes the time-scale parameter that converts the continuous parameters **A** and **B** into the discrete parameters  $\overline{\mathbf{A}}$  and  $\overline{\mathbf{B}}$ ,  $\exp(\cdot)$  denotes the

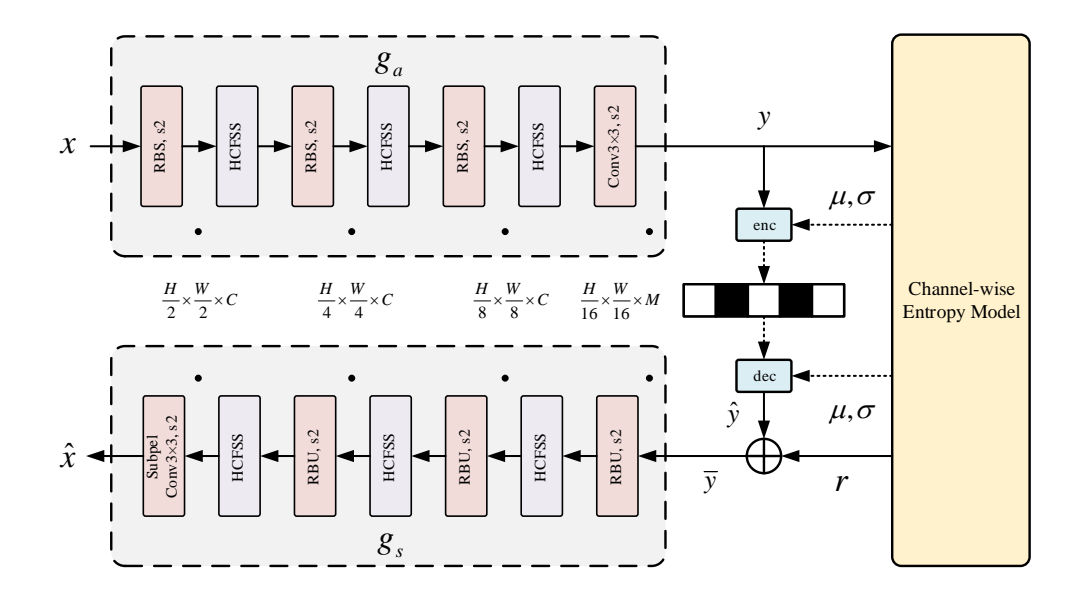


Figure 2: Overall architecture of the proposed HCFSSNet. The HCFSS block denotes the Hybrid Convolution-Frequency State Space block. RBS and RBU denote residual blocks for downsampling and upsampling, respectively, built from  $1\times 1$  and  $3\times 3$  convolutions. "s2" denotes a stride of 2 while "enc" and "dec" denote range encoders/decoders that integrate a quantizer. C and M denote the numbers of channels used for feature extraction and for latent features, respectively.

matrix exponential, and  ${\bf I}$  is the identity matrix. The resulting discrete-time formulation is

$$h_t = \overline{\mathbf{A}} h_{t-1} + \overline{\mathbf{B}} x_t, y_t = \mathbf{C} h_t + \mathbf{D} x_t.$$
 (3)

Mamba [43], as one of the most advanced SSMs, builds on the discrete-time formulation in Eq. 3 and introduces input-dependent selective scanning together with a highly parallel implementation. This design enables Mamba to memorize ultra-long sequences and to extract global features with linear complexity in sequence length, significantly improving both modeling capability and computational efficiency. In this work, we build our visual state space design on such modern SSM formulations and adapt them to two-dimensional image features.

#### 3.2. Problem Formulation

The overall architecture of the proposed HCFSSNet is illustrated in Fig. 2. Formally, given an input image  $\boldsymbol{x}$ , the analysis transform  $g_a$  maps it to latent features  $\boldsymbol{y}$ :

$$\mathbf{y} = g_a(\mathbf{x}; \phi_g), 
\mathbf{z} = h_a(\mathbf{y}; \phi_h), 
\hat{\mathbf{z}} = Q(\mathbf{z} - \mathbf{m}) + \mathbf{m}, 
F_{\text{mean}} = h_{\text{mean}}(\hat{\mathbf{z}}; \theta_{\text{mean}}), 
F_{\text{scale}} = h_{\text{scale}}(\hat{\mathbf{z}}; \theta_{\text{scale}}), 
\bar{\mathbf{y}}_i, \mu_i, \sigma_i = e_i(F_{\text{mean}}, F_{\text{scale}}, \bar{\mathbf{y}}_{< i}, \mathbf{y}_i), \quad 0 \le i < n, 
\hat{\mathbf{x}} = g_s(\bar{\mathbf{y}}; \theta_s),$$
(4)

where  $g_a$  and  $g_s$  denote the analysis and synthesis transforms parameterized by  $\phi_g$  and  $\theta_s$ , respectively;  $h_a$  is the hyper-analysis transform parameterized by  $\phi_h$ ;  $h_{\text{mean}}$  and  $h_{\text{scale}}$  are hyper-synthesis transforms parameterized by  $\theta_{\text{mean}}$ and  $\theta_{\text{scale}}$ ; and  $Q(\cdot)$  denotes a uniform scalar quantizer. The continuous hyperpriors z are centered by subtracting their median m and are then quantized to  $\hat{z}$ .

Throughout the rest of this paper, we use bold lowercase letters (e.g., x) to denote vectors or tensors, and plain letters (e.g.,  $x_{ij}$ ,  $\mu_i$ ,  $\sigma_i$ ) to denote scalars or individual elements.

Following previous works [31, 7], the latent representation  $\boldsymbol{y}$  is divided into n equally sized channel slices  $\{\boldsymbol{y}_0,\boldsymbol{y}_1,\ldots,\boldsymbol{y}_{n-1}\}$  to reduce channel redundancy. For the i-th slice, the channel-wise entropy model  $e_i$  takes as input  $F_{\text{mean}}$ ,  $F_{\text{scale}}$ , the previously reconstructed slices  $\bar{\boldsymbol{y}}_{< i} = \{\bar{\boldsymbol{y}}_0,\ldots,\bar{\boldsymbol{y}}_{i-1}\}$ , and the current slice  $\boldsymbol{y}_i$ , and predicts the refined latent  $\bar{\boldsymbol{y}}_i$  together with its Gaussian parameters  $\mu_i$  and  $\sigma_i$ . The synthesis transform  $g_s$  then reconstructs the final output image  $\hat{\boldsymbol{x}}$  from  $\bar{\boldsymbol{y}} = \{\bar{\boldsymbol{y}}_i\}_{i=0}^{n-1}$ .

In the entropy model, during encoding, the difference between the current slice  $y_i$  and its predicted mean  $\mu_i$  is quantized as

$$\hat{\boldsymbol{y}}_i = Q(\boldsymbol{y}_i - \mu_i) + \mu_i, 
\boldsymbol{r}_i = \operatorname{Res}_i(\mu_i, \hat{\boldsymbol{y}}_i), 
\bar{\boldsymbol{y}}_i = \hat{\boldsymbol{y}}_i + \boldsymbol{r}_i,$$
(5)

where  $\operatorname{Res}_i(\cdot)$  denotes the residual prediction network for the *i*-th slice, which estimates the residual  $\boldsymbol{r}_i$  between  $\boldsymbol{y}_i$  and  $\hat{\boldsymbol{y}}_i$ . Adding  $\boldsymbol{r}_i$  to  $\hat{\boldsymbol{y}}_i$  yields a more accurate reconstruction  $\bar{\boldsymbol{y}}_i$ .

Following Ballé et al. [51], we employ a factorized density model to represent the quantized hyperpriors  $\hat{z}$ :

$$p_{\hat{\boldsymbol{z}}|\boldsymbol{\psi}}(\hat{\boldsymbol{z}} \mid \boldsymbol{\psi}) = \prod_{j} \left( p_{z_{j}|\psi_{j}}(\psi_{j}) * \mathcal{U}\left(-\frac{1}{2}, \frac{1}{2}\right) \right) (\hat{z}_{j}), \tag{6}$$

where  $\psi = \{\psi_j\}$  denotes the hyperprior parameters and  $\mathcal{U}(-\frac{1}{2}, \frac{1}{2})$  models the quantization noise. Similarly, following [45], we model each quantized latent coefficient  $\hat{y}_j$  as a Gaussian distribution with mean  $\mu_j$  and standard deviation  $\sigma_j$ :

$$p_{\hat{\boldsymbol{y}}\mid\hat{\boldsymbol{z}}}(\hat{\boldsymbol{y}}\mid\hat{\boldsymbol{z}},\theta) = \prod_{j} \left( \mathcal{N}(\mu_{j},\sigma_{j}^{2}) * \mathcal{U}\left(-\frac{1}{2},\frac{1}{2}\right) \right) (\hat{y}_{j}), \tag{7}$$

where  $\hat{\boldsymbol{y}} = \{\hat{y}_j\}$  collects all quantized latent coefficients. The integer-valued outputs of the quantizer,  $Q(\boldsymbol{z} - \boldsymbol{m})$  and  $Q(\boldsymbol{y} - \boldsymbol{\mu})$ , are entropy-coded into a bitstream using lossless compression methods such as arithmetic coding. The reconstructed latents are then given by  $\hat{\boldsymbol{z}} = Q(\boldsymbol{z} - \boldsymbol{m}) + \boldsymbol{m}$  and  $\hat{\boldsymbol{y}} = Q(\boldsymbol{y} - \boldsymbol{\mu}) + \boldsymbol{\mu}$ .

To optimize the rate-distortion trade-off in the proposed HCFSSNet, we adopt the following Lagrangian objective:

$$L = R(\hat{\boldsymbol{y}}) + R(\hat{\boldsymbol{z}}) + \lambda D(\boldsymbol{x}, \hat{\boldsymbol{x}})$$

$$= \mathbb{E} \left[ -\log_2 \left( p_{\hat{\boldsymbol{y}}|\hat{\boldsymbol{z}}}(\hat{\boldsymbol{y}} \mid \hat{\boldsymbol{z}}) \right) \right]$$

$$+ \mathbb{E} \left[ -\log_2 \left( p_{\hat{\boldsymbol{z}}|\psi}(\hat{\boldsymbol{z}} \mid \psi) \right) \right]$$

$$+ \lambda D(\boldsymbol{x}, \hat{\boldsymbol{x}}),$$
(8)

where  $\lambda > 0$  is a Lagrange multiplier that controls the trade-off between compression rate and reconstruction quality. The terms  $R(\hat{\boldsymbol{y}})$  and  $R(\hat{\boldsymbol{z}})$  represent the estimated bitrates of  $\hat{\boldsymbol{y}}$  and  $\hat{\boldsymbol{z}}$ , respectively, and  $D(\boldsymbol{x}, \hat{\boldsymbol{x}})$  measures the distortion between the input image  $\boldsymbol{x}$  and the reconstructed image  $\hat{\boldsymbol{x}}$ .

The main paths  $g_a$  and  $g_s$ , together with the hyperprior paths  $h_a$  and  $h_s$ , are composed of  $3 \times 3$  convolutions, sub-pixel  $3 \times 3$  convolutions, residual blocks with stride (RBS), residual block upsampling (RBU) layers, and the proposed Hybrid Convolution–Frequency State Space (HCFSS) block. The RBS, RBU, and sub-pixel convolution layers follow the design of [52]. Details of the HCFSS block are given in Section 3.3.

## 3.3. Hybrid Convolution-Frequency State Space Block

Previous learned image compression methods have predominantly relied on CNN- and Transformer-based architectures, achieving significant progress. More recently, state space models (SSMs) have emerged as a promising alternative in computer vision. In particular, Mamba [43] efficiently captures long-range dependencies with linear complexity, whereas CNNs remain superior at modeling local structures. Liu et al. [7] utilize CNNs to extract local information and Transformers to model long-range dependencies. However, Transformer-based attention incurs high memory consumption and slow inference. In contrast, Mamba-based models can handle long sequences more efficiently, but a backbone built solely on Mamba tends to underutilize local features, which have been shown to be crucial for compression performance [7, 33].

Motivated by these observations, we propose an efficient Hybrid Convolution–Frequency State Space (HCFSS) block that integrates the strengths of CNNs and vision state space models (SSMs) while alleviating their respective limitations. The architecture of the HCFSS block is illustrated in Fig. 3(a). It enhances compression performance by combining local features extracted by a CNN branch with long-range features captured by a Vision Frequency State Space (VFSS) branch.

Given an input feature map  $X \in \mathbb{R}^{C \times H \times W}$ , the HCFSS block first applies a  $1 \times 1$  convolution and then splits the result along the channel dimension into two equal halves, denoted as  $X_{\text{loc}} \in \mathbb{R}^{\frac{C}{2} \times H \times W}$  and  $X_{\text{lr}} \in \mathbb{R}^{\frac{C}{2} \times H \times W}$ :

$$X_{\text{loc}}, X_{\text{lr}} = \text{Split}(\text{Conv}_{1 \times 1}(X)).$$
 (9)

The local branch  $X_{loc}$  is processed by a CNN-based residual network Res(·) to extract local high-frequency details:

$$X'_{\text{loc}} = \text{Res}(X_{\text{loc}}). \tag{10}$$

In parallel, the long-range branch  $X_{lr}$  is fed into the VFSS block to model global contextual information and long-range structures that are typically dominated by low-frequency components:

$$X'_{\rm lr} = VFSS(X_{\rm lr}). \tag{11}$$

The two branches are then concatenated and projected back to C channels via another  $1 \times 1$  convolution:

$$X_{\text{fuse}} = \text{Conv}_{1\times 1} \left( \text{Cat}(X'_{\text{loc}}, X'_{\text{lr}}) \right). \tag{12}$$

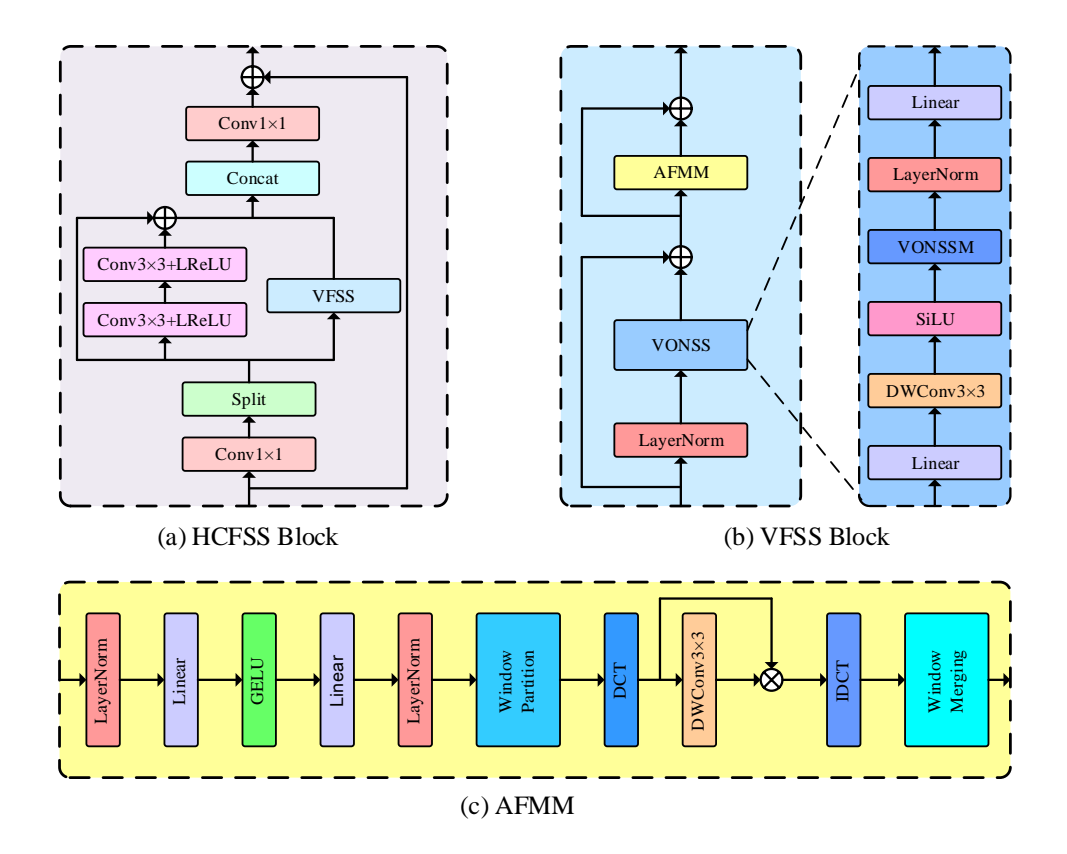


Figure 3: (a) Illustration of the proposed HCFSS block. LReLU denotes the Leaky ReLU activation function. "Split" and "Concat" refer to channel-wise feature separation and concatenation, respectively. VFSS denotes the Vision Frequency State Space block. (b) Architecture of the VFSS block. DwConv denotes depthwise convolution. VONSSM denotes the Vision Omni-directional Neighborhood State Space Module, and AFMM stands for the Adaptive Frequency Modulation Module. (c) Architecture of the AFMM. DCT and IDCT denote the Discrete Cosine Transform and its inverse, respectively.

Finally, a residual connection is added to form the output feature map:

$$X_{\text{output}} = X + X_{\text{fuse}}.$$
 (13)

This design allows HCFSS block to preserve strong local modeling capability while enhancing global contextual modeling via VFSS, without incurring the quadratic complexity of Transformer-based attention.

# 3.4. Vision Frequency State Space Block

To effectively capture long-range dependencies in two-dimensional feature maps, we propose the Vision Frequency State Space (VFSS) block, which consists of a Vision Omni-directional Neighborhood State Space (VONSS) block and an Adaptive Frequency Modulation Module (AFMM). As shown in Fig. 3(b), given an input feature map  $X_{\rm lr}$ , the VFSS block first applies layer normalization and then processes it with VONSS to obtain a long-range informative representation  $X_{\rm VONSS}$ . AFMM subsequently modulates  $X_{\rm VONSS}$  in the frequency domain to preserve compression-critical information while suppressing redundant components. The overall computation can be written as

$$X_{\text{VONSS}} = \text{VONSS}(\text{LN}(X_{\text{lr}})) + X_{\text{lr}},$$
  
 $X'_{\text{lr}} = \text{AFMM}(X_{\text{VONSS}}) + X_{\text{VONSS}}.$  (14)

## 3.4.1. VONSS Block

SSMs were originally designed for one-dimensional sequences; when applied to images, they typically require flattening two-dimensional feature maps into 1D token sequences. This flattening disrupts the positional relationships between adjacent pixels and limits the ability of SSMs to capture spatial structure. For example, Vim [18] employs a single horizontal scan with two directions, so an anchor pixel can only access its immediate left and right neighbors. VMamba [19] extends this idea to both horizontal and vertical scan orders with eight scanning directions, enabling the anchor pixel to access its four nearest axis-aligned neighbors (top, bottom, left, and right). However, VMamba still ignores diagonal neighbors, which also play an important role in preserving local spatial structure.

To address this limitation, we propose the Vision Omni-directional Neighborhood State Space (VONSS) block, which incorporates four types of scanning paths—horizontal, vertical, diagonal, and anti-diagonal—resulting in eight scanning directions. In this way, all first-order neighbors of an anchor pixel are covered, thereby better preserving the local spatial structure of two-dimensional image features.

The VONSS block traverses all possible first-order positional relationships around anchor pixels by leveraging these four scanning paths. Its architecture consists of linear layers, depthwise separable convolution layers, SiLU activation, the VONSS module (VONSSM), and LayerNorm, as illustrated in Fig. 3(b). For a given input feature map  $X_{ln}$ , the processing flow can be

expressed as

$$X_{\text{VONSSM}}^{\text{in}} = \text{SiLU}(\text{DwConv}_{3\times3}(\text{Linear}(X_{\text{ln}}))),$$

$$X_{\text{VONSSM}}^{\text{out}} = \text{VONSSM}(X_{\text{VONSSM}}^{\text{in}}),$$

$$X_{\text{VONSS}}^{\text{out}} = \text{Linear}(\text{LN}(X_{\text{VONSSM}}^{\text{out}})).$$
(15)

As illustrated in Fig. 4, consider pixel 9 and the anchor pixel 13 in the feature map  $X_{\text{VONSSM}}^{\text{in}}$  as an example. Horizontal or vertical scanning alone requires rearranging the feature map into a 1D sequence (e.g., 9-10-11-12-13 or 9-4-23-18-13) when modeling a diagonal direction. This fails to reflect the true spatial proximity between pixels 9 and 13 and significantly distorts the underlying spatial structure. Moreover, as the feature map size increases, the distance between 9 and 13 along the scanning path becomes increasingly inconsistent with their Euclidean distance, which is undesirable for multiscale image compression, where preserving consistent spatial relationships is important.

In contrast, the proposed omni-directional scanning method combines horizontal, vertical, diagonal, and anti-diagonal paths. For instance, pixel 9 can directly connect to pixel 13 via the path 9-13, thereby better preserving local spatial structure and better matching the requirements of image compression and multi-scale feature extraction. Specifically, for a given input feature map  $X_{\text{VONSSM}}^{\text{in}}$ , VONSSM first constructs omni-directional scan sequences using the proposed scanning method, then applies selective state space models (SSMs) [43] along these sequences, and finally merges the results and reshapes them back to a 2D feature map.

#### 3.4.2. Adaptive Frequency Modulation Module

Previous studies [33, 8] have often explicitly decomposed image features into high- and low-frequency components, which are then processed separately to improve rate—distortion performance. In this work, we propose an Adaptive Frequency Modulation Module (AFMM) that operates directly in the DCT domain and data-drivenly learns the relative importance of individual frequency components.

AFMM first transforms local windows of the feature map into the frequency domain using the DCT, and then uses convolutional layers to estimate the relative importance of different frequency coefficients. Compared with explicit decomposition into high- and low-frequency components, the DCT-based representation provides a finer partition of features across frequency components. Moreover, AFMM leverages the anchor pixel and its

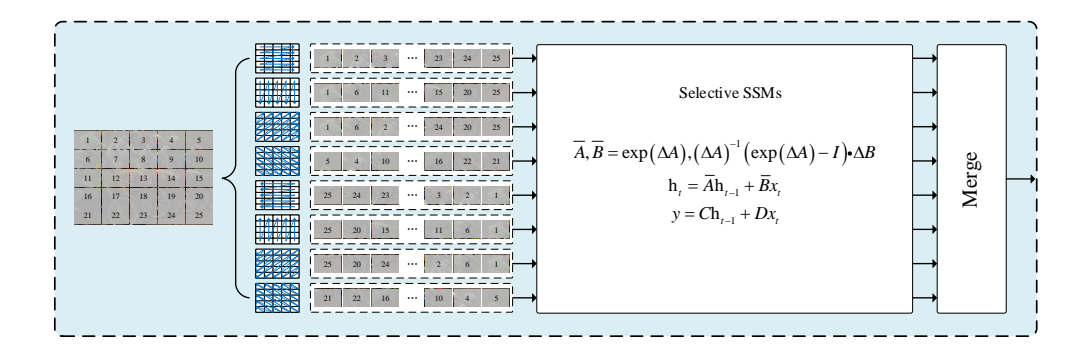


Figure 4: Details of the Vision Omni-directional Neighborhood State Space Module (VON-SSM), illustrating the omni-directional scanning directions.

neighborhood to adaptively enhance or suppress responses at specific spatial locations, so that compression-critical information is retained more effectively while less important details are attenuated.

The structure of AFMM is illustrated in Fig. 3(c). Given an input feature map  $X_{\text{AFMM}}^{\text{in}}$ , AFMM first applies layer normalization and a linear layer to adjust the channel dimension, followed by a GELU activation and another linear layer to restore the original channel dimension. A second layer normalization is then applied:

$$X_{\text{AFMM}}^{\text{act}} = \text{LN}\left(\text{Linear}(\text{GELU}(\text{Linear}(\text{LN}(X_{\text{AFMM}}^{\text{in}}))))\right).$$
 (16)

Next, the feature map is partitioned into non-overlapping windows of size  $w \times w$  by a window-partition operator  $\operatorname{Wp}(\cdot)$ . For each window, the DCT is applied and a  $3 \times 3$  depthwise convolution estimates the importance of each frequency component:

$$F = DCT(Wp(X_{AFMM}^{act})),$$

$$W = Conv_{3\times3}(F).$$
(17)

The resulting weights W are used to modulate the frequency coefficients, which are then transformed back to the spatial domain using inverse DCT (IDCT) and merged by the window-merging operator  $\text{Wm}(\cdot)$ :

$$X_{\text{AFMM}}^{\text{freq}} = \text{Wm}(\text{IDCT}(W \odot F)),$$
 (18)

where  $\odot$  denotes element-wise multiplication. This process enables AFMM to selectively emphasize informative frequency components and suppress less

useful ones, leading to more efficient bit allocation across different frequencies. The effectiveness of VONSS and AFMM is further validated by ablation studies on the Kodak dataset (see Section 4.4).

# 3.5. Channel-wise Entropy Model

Previous studies [33, 53] have shown that substantial redundancy also remains in the entropy modeling stage. By decomposing latent features into high- and low-frequency components and processing them separately, these methods can enhance compression-critical content in the side information while suppressing redundant components, thereby improving overall rate–distortion performance. Motivated by these observations, we design a novel channel-wise entropy model, as illustrated in Fig. 5.

In our model, the latent features  $\boldsymbol{y}$  are first transformed by the hyperanalysis network  $h_a$  into hyperpriors  $\boldsymbol{z}$ , which are encoded using arithmetic coding to produce the side information. The decoded hyperpriors  $\hat{\boldsymbol{z}}$  are then mapped by the hyper-synthesis network  $h_s$  into mean features  $F_{\text{mean}}$  and scale features  $F_{\text{scale}}$ . Both  $h_a$  and  $h_s$  are composed of convolutional layers and HCFSS blocks, allowing them to adaptively modulate information at different frequencies within the side information.

For the *i*-th channel slice, the mean features  $F_{\text{mean}}$ , scale features  $F_{\text{scale}}$ , the current latent slice  $y_i$ , and the previously reconstructed slices  $\{\bar{y}_0, \bar{y}_1, \ldots, \bar{y}_{i-1}\}$  are fed into the slice network  $e_i$  to estimate the mean  $\mu_i$  and scale  $\sigma_i$  of the corresponding encoded feature. Since  $F_{\text{mean}}$  and  $F_{\text{scale}}$  have relatively small spatial resolution and SSMs are more suitable for long sequences, we combine a Swin Transformer block with AFMM to form a Frequency Swin Transformer Attention Module (FSTAM). FSTAM is designed to enhance the estimation of  $\mu_i$  and  $\sigma_i$  by jointly leveraging spatial self-attention and frequency-domain modulation within each window. Finally, each channel slice  $y_i$  is compressed into a bitstream according to a Gaussian distribution parameterized by  $\mu_i$  and  $\sigma_i$ .

#### 4. Experiments

#### 4.1. Experimental Setup

#### 4.1.1. Training Configuration

The network is first pre-trained on 300K images from ImageNet [54] and then fine-tuned on 80K images from LSDIR [55]. For LSDIR, each training sample is randomly cropped to  $512 \times 512$  pixels and the batch size is set to 2.

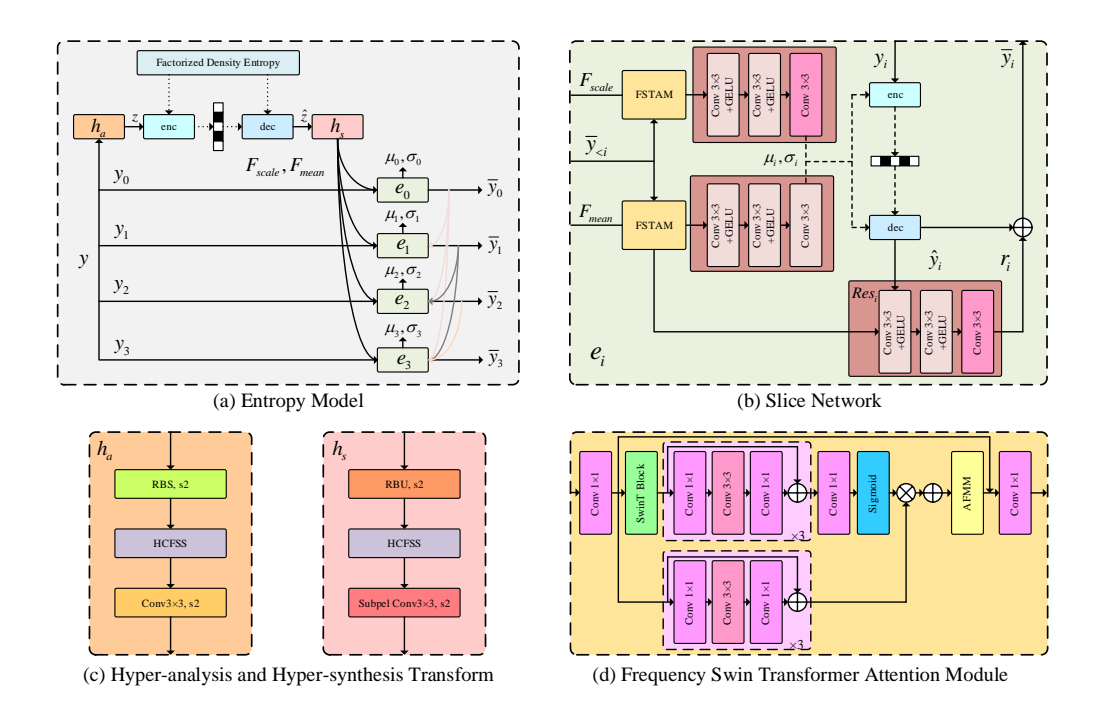


Figure 5: Architectural details of the proposed channel-wise entropy model. (a) Overall structure of the entropy model. (b) Slice network  $e_i$ . (c) Hyper-analysis and hypersynthesis transforms. (d) Frequency Swin Transformer Attention Module (FSTAM); "SwinT block" denotes a Swin Transformer block.

The initial learning rate is  $1\times 10^{-4}$ , which is reduced to  $1\times 10^{-5}$  after 0.4M iterations and further decayed to  $1\times 10^{-6}$  during the final 0.1M iterations. Optimization follows the Lagrangian objective in Eq. 8, with mean-squared error (MSE) used as the distortion metric. The trade-off coefficient  $\lambda$  is set to  $\{0.0025, 0.0035, 0.0067, 0.0130, 0.0250, 0.0500\}$  to obtain models operating at different rate–distortion points. The window size for AFMM in the main HCFSS blocks is set to 16, while FSTAM modules use a window size of 8. All other hyperparameters follow [7]. All models are trained on two NVIDIA RTX 4090 GPUs and evaluated on a single NVIDIA RTX 4090 GPU.

## 4.1.2. Evaluation Protocol

We evaluate the proposed HCFSSNet on three public benchmarks: Kodak (24 images,  $768 \times 512$  pixels) [56], Tecnick (100 images,  $1200 \times 1200$  pixels) [57], and the CLIC Professional Validation set (41 images, approxi-

mately 2K resolution) [58]. Reconstruction fidelity is measured using peak signal-to-noise ratio (PSNR), and the bitrate is reported in bits per pixel (bpp).

# 4.1.3. Model Configuration

The channel width of each HCFSS block is set to 256. Within each HCFSS block, both the VFSS branch and the convolutional branch use 128 channels. The latent representation  $\boldsymbol{y}$  has 320 channels, while the hyperlatent  $\boldsymbol{z}$  has 192 channels. The hyper-analysis and hyper-synthesis transforms are configured with 256 channels. For entropy coding, we adopt a five-slice channel-wise entropy model.

# 4.2. Rate-Distortion Performance

We benchmark HCFSSNet against the conventional VTM anchor and recent state-of-the-art learned codecs, including InvCompress [6], MLIC++ [59], TCM [7], WeConvene [53], CCA [60], FTIC [8], and MambaIC [20]. Figures 6(a)–(c) report PSNR-bitrate curves on Kodak, Tecnick, and the CLIC Professional Validation set, respectively. BD-rate is computed from the PSNR-bitrate curves using the Bjøntegaard method over the common quality range.

Compared with the VTM anchor, the proposed HCFSSNet consistently reduces BD-rate across all three datasets, achieving reductions of 18.06% on Kodak, 24.56% on Tecnick, and 22.44% on CLIC. These gains are observed across the entire rate-distortion range and are particularly noticeable at low-to-medium bitrates, suggesting that HCFSSNet produces more compact latent representations and more accurate probability estimates.

When compared with recent learned codecs, HCFSSNet achieves competitive rate—distortion performance while maintaining a moderate model size and runtime. As summarized in Table 1, HCFSSNet attains BD-rate values comparable to recent high-performing CNN-, Transformer-, and SSM-based codecs, while using substantially fewer parameters than the SSM-based MambaIC and large Transformer-based models such as MLIC++ and WeConvene. Across the three benchmarks, the average BD-rate reduction achieved by HCFSSNet is within about 2 percentage points of that of MambaIC and within 1 percentage point of that of MLIC++, while using 30–35% fewer parameters (80.97M vs. 116.72M and 123.81M, respectively). This indicates that HCFSSNet delivers compression efficiency comparable to the heaviest

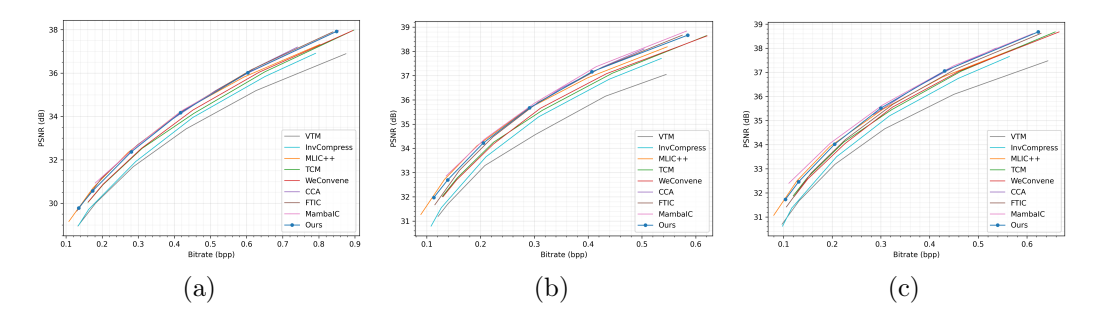


Figure 6: Rate—distortion results (PSNR vs. bitrate, in bpp). From left to right: (a) Kodak, (b) Tecnick, and (c) CLIC Professional Validation. The curves compare state-of-the-art learned image compression methods with the conventional VTM codec; higher PSNR at the same bitrate (or lower bitrate at the same PSNR) indicates better performance.

SSM- and Transformer-based codecs, but with a considerably more compact architecture.

Compared with FTIC [8], which also exploits frequency-aware transforms, HCFSSNet yields markedly better BD-rate performance on high-resolution datasets: on Tecnick and CLIC, our method achieves additional BD-rate reductions of 2.29% and 4.54%, respectively. This suggests that the proposed Hybrid Convolution–Frequency State Space design scales favorably to high-resolution images, where long-range dependencies and fine-grained frequency modeling become more critical. Although HCFSSNet is not the fastest model in terms of runtime, it still provides a significant encoding speed-up over the VTM reference, and its decoding time remains within a practical range for offline and near-real-time applications.

We attribute the competitive performance of HCFSSNet to two key factors. First, the hybrid HCFSS transform decouples the processing of local high-frequency details and long-range low-frequency structures, allowing the two branches to focus on complementary aspects of the signal. Second, the five-slice channel-wise entropy model, enhanced by frequency-aware modeling of the side information, improves the precision of the likelihood estimates without incurring prohibitive decoding cost.

#### 4.3. Visual Results

We further present qualitative comparisons on the Tecnick dataset. Three representative images are selected and compressed using VTM, InvCompress,

Table 1: Complexity and BD-rate (%) comparison between the conventional VTM codec and previous learned image compression methods. BD-rate is measured relative to VTM-23.13 (negative values indicate bitrate savings over VTM).

Method	Params (M)	Enc. (s/img)	Dec. (s/img)	Kodak	Tecnick	CLIC
VTM-23.13	_	70.012	0.189	0.00	0.00	0.00
InvCompress [6]	50.03	1.656	1.758	-5.43	<del>%-10.46</del> %	-8.28%
MLIC++ [59]	116.72	0.016	0.021	-19.24	%-26.11 $%$	-22.71%
TCM [7]	45.18	0.066	0.035	-11.60	%-16.98%	-16.16%
WeConvene [53]	107.15	0.071	0.022	-13.20	%-17.17%	-15.68%
CCA [60]	64.99	0.067	0.063	-18.30	% - 25.99%	-23.25%
FTIC [8]	70.96	0.064	0.052	-19.15	%-22.27%	-17.90%
MambaIC [20]	123.81	0.184	0.177	-18.92	% - 26.84%	-25.98%
Ours	80.97	0.337	0.326	-18.06	% - 24.56%	-22.44%

TCM, WeConvene, FTIC, and the proposed HCFSSNet. The reconstructed images are shown in Fig. 7. As can be seen, HCFSSNet produces reconstructions with sharper edges and finer textures that more closely match the ground-truth images, especially around high-frequency structures such as thin lines and repetitive patterns. This demonstrates that the proposed hybrid transform and frequency-aware entropy model not only improve PSNR, but also preserve visually important details at comparable or lower bitrates.

# 4.4. Ablation Studies

To understand the contribution of each proposed component in HCFSS-Net, we conduct ablation studies on the VONSS block, AFMM, and FSTAM. Unless otherwise stated, all ablation variants are trained on a randomly selected subset of 100K images from the training set (resolution  $\geq 256 \times 256$ ) with a batch size of 8, and evaluated on the Kodak dataset.

## 4.4.1. Effectiveness of the VONSS Block

We first examine the impact of the proposed VONSS block. To this end, we compare a variant of our model that uses VONSS with another variant in which VONSS is replaced by the Cross-Scan Module (CSM) proposed in VMamba [19]. For a fair comparison, both variants are trained without AFMM and FSTAM. As shown in Fig. 8(a), the model equipped with VONSS consistently outperforms the CSM-based variant across the tested range of bitrates. This improvement stems from VONSS's ability to preserve complete



Figure 7: Visual comparisons on the Tecnick dataset [57]. Compared with the other methods, the proposed HCFSSNet preserves more structural details at lower bitrates. Please zoom in for a cleaner view.

local neighborhood structures—including diagonal neighbors—when applying state space models to 2D feature maps, which in turn facilitates more accurate modeling of long-range dependencies for compression.

On the Kodak dataset, at three operating points around 0.45, 0.65, and 0.92 bpp, replacing CSM with VONSS increases PSNR from 34.11 to 34.16 dB, from 35.73 to 35.83 dB, and from 37.75 to 37.90 dB, respectively, while the bitrate remains nearly unchanged (within 0.001–0.007 bpp). This indicates that preserving omni-directional neighborhoods is beneficial for state-space-based transforms on 2D feature maps.

In this experiment, both models are trained from scratch on 300K randomly selected images from ImageNet, each with a minimum resolution of  $256 \times 256$ , and are evaluated on the Kodak dataset.

#### 4.4.2. Effectiveness of the AFMM

Given the positive contribution of VONSS, we next assess the effect of AFMM. Starting from the VONSS-based variant, we add AFMM to form the full VFSS block and compare it against the baseline without AFMM. The results in Fig. 8(b) show that incorporating AFMM further improves the

rate—distortion performance. This improvement arises because AFMM operates in the DCT domain to perform fine-grained, content-adaptive weighting of different frequency components, effectively allocating more bits to compression-critical frequencies while suppressing redundant ones. As a result, the model achieves a better balance between bitrate and reconstruction quality.

More concretely, on the Kodak dataset, at three operating points around 0.47, 0.69, and 1.01 bpp, adding AFMM improves PSNR from 33.64 to 33.73 dB, from 35.30 to 35.52 dB, and from 37.16 to 37.35 dB, respectively, while slightly reducing the bitrate from 0.475 to 0.465 bpp, from 0.688 to 0.682 bpp, and from 1.007 to 0.968 bpp. This corresponds to roughly 1–4% rate savings at similar quality and confirms that DCT-domain adaptive frequency modulation leads to a better rate-distortion trade-off.

## 4.4.3. Effectiveness of the FSTAM

Finally, we evaluate the proposed FSTAM within the entropy model. We compare a variant that uses FSTAM against another variant in which FSTAM is replaced by the Swin-based attention module (SWAtten) from [7]. As shown in Fig. 8(c), the FSTAM-based model consistently achieves better rate—distortion performance than the SWAtten-based counterpart. This confirms that combining a Swin Transformer block with AFMM in the hyperprior pathway is more effective at reducing spatial redundancy in side information and improving the accuracy of the estimated Gaussian parameters  $(\mu_i, \sigma_i)$  for each channel slice.

At two operating points around 0.68 and 0.97 bpp on the Kodak dataset, replacing SWAtten with FSTAM increases PSNR from 35.52 to 35.56 dB and from 37.35 to 37.43 dB, respectively, while keeping the bitrate virtually unchanged (0.682 vs. 0.680 bpp and 0.968 vs. 0.969 bpp). Although the numerical gains are modest (about 0.04–0.08 dB), they are consistent across the tested operating points, which indicates that frequency-aware attention is more effective for modeling side information.

Overall, the ablation results in Fig. 8 indicate that VONSS, AFMM, and FSTAM contribute complementary gains. VONSS mainly helps SSM-based transforms better preserve the 2D neighborhood structure by jointly modeling horizontal, vertical, and diagonal contexts, AFMM brings additional BD-rate savings via fine-grained frequency modulation, and FSTAM further enhances side-information modeling.

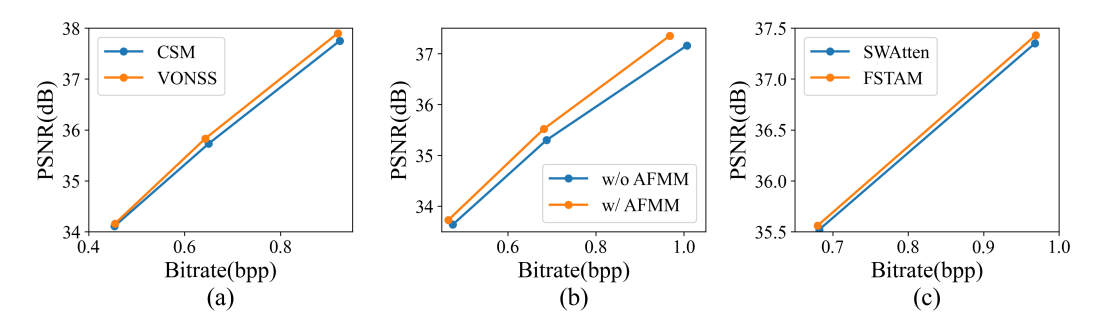


Figure 8: Ablation studies on the Kodak dataset. (a) comparison between the Cross-Scan Module (CSM) and the proposed VONSS block; (b) ablation of the AFMM, where "w/" denotes "with" and "w/o" denotes "without"; and (c) comparison between the Swin-based attention module (SWAtten) and the proposed FSTAM.

#### 4.5. Discussion

It is worth noting that some very recent LIC models, including MambaIC [20], DCAE [34], and LALIC [35], report even lower BD-rate than HCFSSNet on certain benchmarks. MambaIC forms a deep visual state space architecture by inserting SSM blocks throughout both the main and hyperprior transforms, whereas DCAE introduces a dictionary-based cross-attention entropy model with multi-scale feature aggregation, leading to a computationally heavy entropy module and a large overall model size (about 119M parameters). LALIC, in contrast, is a Bi-RWKV-based codec with linear attention and an RWKV-based spatial—channel context model, achieving competitive BD-rate with a moderate parameter budget (around 63M parameters) and decoding latency.

In this context, our goal is not to aggressively push BD-rate to the absolute minimum by using ever larger models or increasingly specialized attention modules. Instead, HCFSSNet deliberately adopts a moderate model size (80.97M parameters) and a unified hybrid design that tightly couples omnidirectional visual state space modeling with fine-grained frequency-domain modulation in both the main transform and the entropy model. As summarized in Table 1, our method achieves a competitive rate-distortion trade-off while using noticeably fewer parameters than MambaIC and several large Transformer-based codecs. We therefore view HCFSSNet as a compact and extensible backbone that can serve as a foundation for future high-capacity variants, rather than a competitor that aims to strictly dominate all existing methods in terms of absolute BD-rate.

Overall, these observations suggest that recent trends in learned image

compression are diverging into two directions: performance-oriented architectures that push BD-rate with increasingly sophisticated sequence and context modules, and more unified, modular designs that emphasize efficiency and extensibility. HCFSSNet follows the latter direction and thus complements, rather than directly competing with, large-capacity or highly specialized codecs like MambaIC, DCAE, and LALIC. While these models explore a different part of the design space—using heavier entropy modules, deeper SSM or linear-attention stacks, or complex latent interaction mechanisms—our results indicate that a unified spatial–frequency SSM framework can already achieve competitive rate—distortion trade-offs at a moderate model size, while maintaining architectural clarity and offering a scalable foundation for future extensions.

## 5. Conclusion

This work presents a novel learned image compression framework, Hybrid Convolution and Frequency State Space Network (HCFSSNet), which combines the complementary strengths of convolutional neural networks (CNNs) and state space models (SSMs). In the main transform, the proposed Hybrid Convolution-Frequency State Space (HCFSS) block decouples local and long-range processing via a dual-branch design: a CNN branch focuses on local high-frequency structures, while the Vision Frequency State Space (VFSS) branch—equipped with the omni-directional VONSS block and the Adaptive Frequency Modulation Module (AFMM)—captures long-range dependencies and performs content-aware frequency shaping. In the entropy model, we further introduce the Frequency Swin Transformer Attention Module (FSTAM) to enhance side-information modeling and mitigate channel-wise redundancy.

Extensive experiments on the Kodak, Tecnick, and CLIC Professional Validation datasets show that HCFSSNet consistently reduces BD-rate with respect to the conventional VTM anchor and achieves rate—distortion performance that is competitive with recent CNN-, Transformer-, and SSM-based learned codecs, while using fewer parameters than large Transformer-based and Mamba-based models. Compared with the frequency-aware FTIC codec, HCFSSNet yields notable BD-rate gains on high-resolution datasets, indicating that the Hybrid Convolution—Frequency State Space design scales favorably to large images. We believe that the proposed hybrid architecture, which unifies omni-directional visual state space modeling and frequency-domain modulation in both the main transform and the entropy model, pro-

vides a compact and interpretable foundation that can be further extended to higher-capacity models, real-time scenarios, and other modalities such as video compression.

In future work, we plan to explore lighter variants of HCFSSNet for realtime and resource-constrained scenarios, and to extend the framework to video compression and other modalities in which long-range dependencies and frequency structure are equally critical.

#### References

- [1] G. Wallace, The jpeg still picture compression standard, IEEE Transactions on Consumer Electronics 38 (1) (1992) xviii–xxxiv. doi:10.1109/30.125072.
- [2] A. Skodras, C. Christopoulos, T. Ebrahimi, The jpeg 2000 still image compression standard, IEEE Signal Processing Magazine 18 (5) (2001) 36–58. doi:10.1109/79.952804.
- [3] G. Ginesu, M. Pintus, D. D. Giusto, Objective assessment of the webp image coding algorithm, Signal processing: image communication 27 (8) (2012) 867–874.
- [4] F. Bellard, Bpg image format, http://bellard.org/bpg/, accessed: Oct. 30, 2018 (2014).
- [5] B. Bross, Y.-K. Wang, Y. Ye, S. Liu, J. Chen, G. J. Sullivan, J.-R. Ohm, Overview of the versatile video coding (vvc) standard and its applications, IEEE Transactions on Circuits and Systems for Video Technology 31 (10) (2021) 3736–3764.
- [6] Y. Xie, K. L. Cheng, Q. Chen, Enhanced invertible encoding for learned image compression, in: Proceedings of the ACM International Conference on Multimedia, 2021, pp. 162–170.
- [7] J. Liu, H. Sun, J. Katto, Learned image compression with mixed transformer-cnn architectures, in: Proceedings of the IEEE/CVF conference on computer vision and pattern recognition, 2023, pp. 14388–14397.

- [8] H. Li, S. Li, W. Dai, C. Li, J. Zou, H. Xiong, Frequency-aware transformer for learned image compression, in: The Twelfth International Conference on Learning Representations, 2024.

  URL https://openreview.net/forum?id=HKGQDDTuvZ
- [9] C. E. Shannon, A mathematical theory of communication, The Bell System Technical Journal 27 (3) (1948) 379–423. doi:10.1002/j.1538-7305.1948.tb01338.x.
- [10] D. P. Kingma, M. Welling, Auto-Encoding Variational Bayes, in: 2nd International Conference on Learning Representations, ICLR 2014, Banff, AB, Canada, April 14-16, 2014, Conference Track Proceedings, 2014. arXiv:http://arxiv.org/abs/1312.6114v10.
- [11] J. Rissanen, G. Langdon, Universal modeling and coding, IEEE Transactions on Information Theory 27 (1) (1981) 12–23. doi:10.1109/TIT.1981.1056282.
- [12] G. N. N. Martin, Range encoding: an algorithm for removing redundancy from a digitised message, in: Proc. Institution of Electronic and Radio Engineers International Conference on Video and Data Recording, Vol. 2, 1979.
- [13] T. Chen, H. Liu, Z. Ma, Q. Shen, X. Cao, Y. Wang, End-to-end learnt image compression via non-local attention optimization and improved context modeling, IEEE Transactions on Image Processing 30 (2021) 3179–3191. doi:10.1109/TIP.2021.3058615.
- [14] Y. Zhu, Y. Yang, T. Cohen, Transformer-based transform coding, in: International Conference on Learning Representations, 2022. URL https://openreview.net/forum?id=IDwN6xjHnK8
- [15] S. Qin, J. Wang, Y. Zhou, B. Chen, T. Luo, B. An, T. Dai, S. Xia, Y. Wang, Mambavc: Learned visual compression with selective state spaces, arXiv preprint arXiv:2405.15413 (2024).
- [16] Z. Liu, Y. Lin, Y. Cao, H. Hu, Y. Wei, Z. Zhang, S. Lin, B. Guo, Swin transformer: Hierarchical vision transformer using shifted windows, in: Proceedings of the IEEE/CVF International Conference on Computer Vision (ICCV), 2021.

- [17] H. Wei, Y. Zhou, Y. Jia, C. Ge, S. Anwar, A. Mian, A lightweight model for perceptual image compression via implicit priors, Neural Networks (2025) 108279.
- [18] L. Zhu, B. Liao, Q. Zhang, X. Wang, W. Liu, X. Wang, Vision mamba: Efficient visual representation learning with bidirectional state space model, in: Forty-first International Conference on Machine Learning, 2024.
- [19] Y. Liu, Y. Tian, Y. Zhao, H. Yu, L. Xie, Y. Wang, Q. Ye, J. Jiao, Y. Liu, VMamba: Visual state space model, in: The Thirty-eighth Annual Conference on Neural Information Processing Systems, 2024. URL https://openreview.net/forum?id=ZgtLQQR1K7
- [20] F. Zeng, H. Tang, Y. Shao, S. Chen, L. Shao, Y. Wang, Mambaic: State space models for high-performance learned image compression, in: Proceedings of the Computer Vision and Pattern Recognition Conference, 2025, pp. 18041–18050.
- [21] D. Minnen, J. Ballé, G. D. Toderici, Joint autoregressive and hierarchical priors for learned image compression, Advances in neural information processing systems 31 (2018).
- [22] J. Zhou, Multi-scale and context-adaptive entropy model for image compression, in: Proceedings of the IEEE/CVF Conference on Computer Vision and Pattern Recognition (CVPR) Workshops, 2019.
- [23] Z. Cui, J. Wang, S. Gao, T. Guo, Y. Feng, B. Bai, Asymmetric gained deep image compression with continuous rate adaptation, in: Proceedings of the IEEE/CVF Conference on Computer Vision and Pattern Recognition (CVPR), 2021, pp. 10532–10541.
- [24] A. v. d. Oord, N. Kalchbrenner, O. Vinyals, L. Espeholt, A. Graves, K. Kavukcuoglu, Conditional image generation with pixelcnn decoders, in: Proceedings of the 30th International Conference on Neural Information Processing Systems, NIPS'16, Curran Associates Inc., Red Hook, NY, USA, 2016, p. 4797–4805.
- [25] J. Devlin, M.-W. Chang, K. Lee, K. Toutanova, BERT: Pre-training of deep bidirectional transformers for language understanding, in:

- J. Burstein, C. Doran, T. Solorio (Eds.), Proceedings of the 2019 Conference of the North American Chapter of the Association for Computational Linguistics: Human Language Technologies, Volume 1 (Long and Short Papers), Association for Computational Linguistics, Minneapolis, Minnesota, 2019, pp. 4171–4186. doi:10.18653/v1/N19-1423. URL https://aclanthology.org/N19-1423
- [26] C. R. Qi, H. Su, M. Nießner, A. Dai, M. Yan, L. J. Guibas, Volumetric and multi-view cnns for object classification on 3d data, in: 2016 IEEE Conference on Computer Vision and Pattern Recognition (CVPR), 2016, pp. 5648–5656. doi:10.1109/CVPR.2016.609.
- [27] S. Ji, W. Xu, M. Yang, K. Yu, 3d convolutional neural networks for human action recognition, IEEE transactions on pattern analysis and machine intelligence 35 (1) (2012) 221–231.
- [28] T. Chen, H. Liu, Z. Ma, Q. Shen, X. Cao, Y. Wang, End-to-end learnt image compression via non-local attention optimization and improved context modeling, IEEE Transactions on Image Processing 30 (2021) 3179–3191. doi:10.1109/TIP.2021.3058615.
- [29] F. Mentzer, E. Agustsson, M. Tschannen, R. Timofte, L. V. Gool, Conditional probability models for deep image compression, in: 2018 IEEE/CVF Conference on Computer Vision and Pattern Recognition, 2018, pp. 4394–4402. doi:10.1109/CVPR.2018.00462.
- [30] Z. Tang, H. Wang, X. Yi, Y. Zhang, S. Kwong, C.-C. J. Kuo, Joint graph attention and asymmetric convolutional neural network for deep image compression, IEEE Transactions on Circuits and Systems for Video Technology 33 (1) (2023) 421–433. doi:10.1109/TCSVT.2022.3199472.
- [31] D. Minnen, S. Singh, Channel-wise autoregressive entropy models for learned image compression, in: 2020 IEEE International Conference on Image Processing (ICIP), IEEE, 2020, pp. 3339–3343.
- [32] D. He, Z. Yang, W. Peng, R. Ma, H. Qin, Y. Wang, Elic: Efficient learned image compression with unevenly grouped space-channel contextual adaptive coding, in: Proceedings of the IEEE/CVF Conference on Computer Vision and Pattern Recognition, 2022, pp. 5718–5727.

- [33] J. Wang, Q. Ling, Fdnet: Frequency decomposition network for learned image compression, IEEE Transactions on Circuits and Systems for Video Technology 34 (11) (2024) 11241–11255. doi:10.1109/TCSVT.2024.3415823.
- [34] J. Lu, L. Zhang, X. Zhou, M. Li, W. Li, S. Gu, Learned image compression with dictionary-based entropy model, in: Proceedings of the Computer Vision and Pattern Recognition Conference, 2025, pp. 12850–12859.
- [35] D. Feng, Z. Cheng, S. Wang, R. Wu, H. Hu, G. Lu, L. Song, Linear attention modeling for learned image compression, in: Proceedings of the Computer Vision and Pattern Recognition Conference, 2025, pp. 7623–7632.
- [36] J. Ballé, V. Laparra, E. P. Simoncelli, End-to-end optimized image compression, in: International Conference on Learning Representations, 2017. URL https://openreview.net/forum?id=rJxdQ3jeg
- [37] Z. Zhang, S. Esenlik, Y. Wu, M. Wang, K. Zhang, L. Zhang, End-to-end learning-based image compression with a decoupled framework, IEEE Transactions on Circuits and Systems for Video Technology 34 (5) (2024) 3067–3081. doi:10.1109/TCSVT.2023.3313974.
- [38] A. Vaswani, N. Shazeer, N. Parmar, J. Uszkoreit, L. Jones, A. N. Gomez, L. Kaiser, I. Polosukhin, Attention is all you need, in: Proceedings of the 31st International Conference on Neural Information Processing Systems, NIPS'17, Curran Associates Inc., Red Hook, NY, USA, 2017, p. 6000–6010.
- [39] R. Zou, C. Song, Z. Zhang, The devil is in the details: Window-based attention for image compression, in: Proceedings of the IEEE/CVF Conference on Computer Vision and Pattern Recognition (CVPR), 2022, pp. 17492–17501.
- [40] M. Lu, P. Guo, H. Shi, C. Cao, Z. Ma, Transformer-based image compression, in: 2022 Data Compression Conference (DCC), 2022, pp. 469–469. doi:10.1109/DCC52660.2022.00080.

- [41] J. Wang, Q. Ling, Fdnet: Frequency decomposition network for learned image compression, IEEE Transactions on Circuits and Systems for Video Technology 34 (11) (2024) 11241–11255. doi:10.1109/TCSVT.2024.3415823.
- [42] Z. Ge, S. Ma, W. Gao, J. Pan, C. Jia, Nlic: Non-uniform quantization-based learned image compression, IEEE Transactions on Circuits and Systems for Video Technology 34 (10) (2024) 9647–9663. doi:10.1109/TCSVT.2024.3401872.
- [43] A. Gu, T. Dao, Mamba: Linear-time sequence modeling with selective state spaces, in: First Conference on Language Modeling, 2024. URL https://openreview.net/forum?id=tEYskw1VY2
- [44] Y. Xiao, Y. Xia, Pixel adaptive deep unfolding network with state space model for image deraining, Neural Networks (2025) 107845.
- [45] J. Ballé, D. Minnen, S. Singh, S. J. Hwang, N. Johnston, Variational image compression with a scale hyperprior, in: International Conference on Learning Representations, 2018.

  URL https://openreview.net/forum?id=rkcQFMZRb
- [46] D. He, Y. Zheng, B. Sun, Y. Wang, H. Qin, Checkerboard context model for efficient learned image compression, in: Proceedings of the IEEE/CVF Conference on Computer Vision and Pattern Recognition, 2021, pp. 14771–14780.
- [47] Y. Wang, H. Fu, Q. Cao, S. Wang, Z. Chen, F. Liang, S2lic: Learned image compression with the swinv2 block, adaptive channel-wise and global-inter attention context, Neural Networks (2025) 107590.
- [48] D. Li, Y. Bai, K. Wang, J. Jiang, X. Liu, W. Gao, Groupedmixer: An entropy model with group-wise token-mixers for learned image compression, IEEE Transactions on Circuits and Systems for Video Technology 34 (10) (2024) 9606–9619. doi:10.1109/TCSVT.2024.3395481.
- [49] T. Yao, Y. Pan, Y. Li, C.-W. Ngo, T. Mei, Wave-vit: Unifying wavelet and transformers for visual representation learning, in: European Conference on Computer Vision, Springer, 2022, pp. 328–345.

- [50] S. Tang, H. Zhang, X. Gao, S. Yang, J. Leng, Z. Pan, H. Tian, A spatial-frequency hybrid restoration network for jpeg compressed image deblurring, Neural Networks (2025) 108059.
- [51] J. Ballé, V. Laparra, E. P. Simoncelli, Density modeling of images using a generalized normalization transformation, in: Y. Bengio, Y. LeCun (Eds.), 4th International Conference on Learning Representations, ICLR 2016, San Juan, Puerto Rico, May 2-4, 2016, Conference Track Proceedings, 2016.
  URL http://arxiv.org/abs/1511.06281
- [52] Z. Cheng, H. Sun, M. Takeuchi, J. Katto, Learned image compression with discretized gaussian mixture likelihoods and attention modules, in: Proceedings of the IEEE Conference on Computer Vision and Pattern Recognition (CVPR), 2020.
- [53] H. Fu, J. Liang, Z. Fang, J. Han, F. Liang, G. Zhang, Weconvene: Learned image compression with wavelet-domain convolution and entropy model (2024). arXiv:2407.09983. URL https://arxiv.org/abs/2407.09983
- [54] J. Deng, W. Dong, R. Socher, L.-J. Li, K. Li, L. Fei-Fei, Imagenet: A large-scale hierarchical image database, in: 2009 IEEE conference on computer vision and pattern recognition, Ieee, 2009, pp. 248–255.
- [55] Y. Li, K. Zhang, J. Liang, J. Cao, C. Liu, R. Gong, Y. Zhang, H. Tang, Y. Liu, D. Demandolx, et al., Lsdir: A large scale dataset for image restoration, in: Proceedings of the IEEE/CVF Conference on Computer Vision and Pattern Recognition, 2023, pp. 1775–1787.
- [56] E. Kodak, Kodak lossless true color image suite (photocd pcd0992), URL http://r0k. us/graphics/kodak 6 (1993) 2.
- [57] N. Asuni, A. Giachetti, et al., Testimages: a large-scale archive for testing visual devices and basic image processing algorithms., in: STAG, 2014, pp. 63–70.
- [58] G. Toderici, W. Shi, R. Timofte, L. Theis, J. Ballé, E. Agustsson, N. Johnston, F. Mentzer, Clic: Workshop and challenge on learned image compression, in: Proc. IEEE/CVF Conf. Comput. Vis. Pattern Recognit, 2020.

- [59] W. Jiang, R. Wang, Mlic++: Linear complexity multi-reference entropy modeling for learned image compression, in: ICML 2023 Workshop Neural Compression: From Information Theory to Applications, 2023. URL https://openreview.net/forum?id=hxIpcSoz2t
- [60] M. Han, S. Jiang, S. Li, X. Deng, M. Xu, C. Zhu, S. Gu, Causal context adjustment loss for learned image compression, Advances in Neural Information Processing Systems 37 (2024) 133231–133253.